Available online at www.sciencedirect.com
SCIENCE DIRECT
Earth and Planetary Science Letters 246 (2006) 393–406
EPSL
www.elsevier.com/locate/epsl

Temporal record of lithium in seawater: A tracer for silicate weathering?

Ed C. Hathorne *, Rachael H. James

Centre for Earth, Planetary, Space and Astronomical Research, The Open University, Milton Keynes MK7 6AA, UK

Received 5 September 2005; received in revised form 22 March 2006; accepted 13 April 2006
Available online 30 May 2006
Editor: H. Elderfield

Abstract

This paper presents multi-species records of the Li/Ca ratio and Li isotopic composition (δ^7Li) of planktonic foraminifera from the Pacific and Atlantic oceans for the past 18 Ma. The Li/Ca record is corrected for interspecific offsets determined from recent (Holocene) foraminifera; interspecific offsets in δ^7Li are not significant. Despite different diagenetic histories, the records produced from both oceans are remarkably consistent. Corrected planktonic foraminiferal Li/Ca ratios range from 6.3 to 10.9 μmol/mol, while planktonic foraminiferal δ^7Li ranges from 25 to 31‰. Both records are interpreted in terms of long-term changes in seawater Li/Ca and δ^7Li, enabling issues related to higher-resolution variability in Li/Ca and δ^7Li to be ignored. By assuming that the hydrothermal flux of Li into the oceans, and the flux of Li removed from the oceans during low-temperature uptake by marine basalts and sediments, have not changed significantly since 18 Ma, and using published records for the seawater calcium concentration, the seawater Li/Ca and δ^7Li records can be used to estimate global average river δ^7Li and Li fluxes. Our records indicate that the river flux of dissolved Li decreased between 16 and ~8 Ma while the δ^7Li value of the river input increased. These data imply that both silicate weathering rates and weathering intensity decreased over this interval which may have been responsible for putative increases in levels of atmospheric CO_2. In contrast, the riverine flux of Li has increased since ~8 Ma while its δ^7Li value has increased. This implies that the silicate weathering rate has increased, while weathering intensity has decreased, since that time.

Keywords: Li isotopes; planktonic foraminifera; paleoceanography; silicate weathering; atmospheric CO_2

1. Introduction

Many lines of evidence, from both marine and terrestrial records, suggest that there have been dramatic changes in the Earth's climate system during the last 65 Myr that occur on both long (i.e., $>10^5$ yr) and short time scales (e.g. [1,2]). The mechanisms that are responsible for these changes are less well established, but there is growing evidence that amongst the primary controls is the concentration of atmospheric carbon dioxide (e.g. [2,3]).

On time scales of $>10^5$ yrs variations in atmospheric CO_2 are primarily induced by imbalance between mantle degassing and chemical weathering of continental silicate rocks. Thus far information on past changes in silicate weathering rates largely relies on studies of the temporal record of the Sr isotopic composition of the

* Corresponding author. Tel.: +44 1908 659781; fax: +44 1908 655151.
E-mail addresses: E.C.Hathorne@open.ac.uk (E.C. Hathorne), R.H.James@open.ac.uk (R.H. James).

0012-821X/$ - see front matter © 2006 Elsevier B.V. All rights reserved.
doi:10.1016/j.epsl.2006.04.020

oceans; for example, the pronounced increase since 40 Ma ago in seawater $^{87}Sr/^{86}Sr$ (e.g. [4]) has been linked to increased uplift and erosion (and hence increased weathering) due to initiation of the Himalayan orogeny at ~50 Ma [5], and to long-term cooling within the Cenozoic (the change from a 'greenhouse' to an 'icehouse' world). However, in recent years, the utility of this proxy has been questioned, largely because shifts in Sr isotopes may reflect changes in the composition of the continental source rather than a simple change in weathering flux (e.g. [6]). To better constrain the links between weathering and climate, it is therefore imperative to find new proxies for continental silicate weathering.

Lithium is one potential proxy. Li is conservative in the ocean, with a residence time of about a million years [7,8], and it is isotopically uniform on a global scale ($\delta^7Li = +31‰$ [9]). The Li concentration and Li isotopic composition of seawater is maintained by inputs of high-temperature hydrothermal fluids at oceanic ridges (with $\delta^7Li \sim +6.7‰$ [10]) and dissolved Li from rivers (with average $\delta^7Li \sim +23‰$ [8]), and low-temperature removal of Li into oceanic basalts and marine sediments (Table 1). Uptake of Li into marine sediments occurs mainly via sorption to clays [11]; carbonates incorporate relatively little Li [12]. Thus, seawater Li is heavier than its sources and this is maintained by preferential removal of ^6Li during low-temperature alteration. The average isotopic fractionation factor between basalt/sediment and seawater (α) is ~0.985 [10,13,14].

Table 1
Oceanic Li budget. Values used for mass balance calculations are shown in bold

	Flux (10^9 mol/yr)	References
Input		
High temperature hydrothermal fluids	3–15	[20,21]
	6	
Rivers	8–16	[8,20]
	8	
Fluid expulsion at convergent margins	0.08– 0.6 [a]	[22,23]
Output		
Low temperature alteration of basalt	1–12	[20,21,25,26]
	10	
Uptake into marine sediments	3.5 – 37	[11,20]
	4	
Atmospheric cycling	0.14	[20]
Uptake into biogenic carbonates	0.3–0.9	[12]
Uptake into biogenic silica	0.08	[27]

[a] Far higher values ($10–30 \times 10^9$ mol/yr) are reported by Martin et al. [24]. These were calculated using a global water expulsion flux of 100 $km^3\ yr^{-1}$which is based on fluid flow rates. This water expulsion flux is at least two orders of magnitude higher than those calculated on the basis of: (i) dewatering of subducted sediments [28]; (ii) heat flow patterns [29]; and (iii) flow meter measurements [30]. We discount the former value here because it is likely that it is affected by external sources of fluid (e.g. seawater, meteoric water) or transient high flow rates [31].

Until recently, relatively little was know about the behaviour of Li during continental weathering. In a study of some of the world's major rivers, Huh et al. [8] noted that the important processes affecting the lithium isotopic compositions of the dissolved load are isotopic fractionation between solution and secondary minerals and the degree of weathering, and overlain on this is the effect of the bedrock type. In a later study, Huh et al. [15] reported that the dissolved load of tributaries of the Orinoco was systematically isotopically heavier than the corresponding suspended load; during weathering, ^6Li is concentrated in alteration products and ^7Li goes preferentially into solution. Preferential retention of ^6Li in secondary minerals is also observed during weathering of soils [16]. Huh et al. [15] also noted that, to a first approximation, as weathering intensity (as defined, for example, by the chemical index of alteration; [17]) increased the δ^7Li value of the dissolved load approached that of the suspended load. Similarly, the δ^7Li value of rivers draining basalts in Iceland decreases with age since eruption [18]. Finally, recent work conducted in the Himalaya indicates that >90% of dissolved Li in rivers is derived from weathering of silicates, even in carbonate-dominated catchments [19]; importantly, this suggests that changes in the continental flux of Li largely reflect changes in silicate weathering rates.

To date, there is just one report of the past variation in seawater Li [7] and one report of the past variation in seawater δ^7Li [12] on time scales of $>10^5$ yrs. The former suggests that there has been little change in seawater Li since 40 Ma, while the latter reports large variations in seawater δ^7Li (from +11 to +31‰) over the same period. These studies imply a major and rapid change in the river input: the δ^7Li value shifting from +23‰ (present-day) to ca. −12‰, which is implausible as the lowest δ^7Li value for any river sampled to date is +6‰ [8]. A large part of this discrepancy may be due to the poor quality of the data being derived from multiple foraminifera species using now outdated analytical techniques. To this end, we have produced new Li and Li isotope records from analyses of planktonic foraminifera using greatly improved methodology. First, we utilise only single species foraminifera to account for interspecific effects (e.g. [32]). Secondly, we restrict the size of the foraminifera tests to the >355 μm fraction to

minimise any 'growth rate' effect resulting from variations in seawater carbonate ion concentration ($[CO_3^{2-}]$) [33]. Thirdly, we use chemical cleaning to remove surface contamination from the foraminifera tests, and finally we utilise improved techniques for the measurement of Li isotopes in low concentration natural samples (e.g. [34]).

2. Materials and methods

Recent foraminifera were picked from the uppermost 2 cm of sediments recovered by box-cores deployed in the north Atlantic. Most of these foraminifera were extracted from sediments that contained abundant pterapod shells; this suggests that the foraminifera tests are unlikely to have undergone dissolution as aragonite is more soluble than calcite [35]. Ancient foraminifera were picked from sediments supplied by the Ocean Drilling Program from the western equatorial Pacific (ODP Site 871, 5.3°N, 172.2°E and ODP Site 872, 10.6°N, 162.5°E) and the subtropical south Atlantic (ODP Site 1264, 28.3°S, 2.5°E). Chronology for Sites 871 and 872 was derived from planktonic foraminifera stratigraphy [36], while chronology for Site 1264 was determined from a combined biostratigraphic/paleomagnetic age model [37]. The preservation state of the ancient foraminifera varied between the different locations, and down-core. Material from Site 1264 has clearly undergone some recrystallization as evident from increasing down-core pore water Sr^{2+} concentrations [37]. Visual inspection of the foraminifera tests under light and scanning electron microscopy suggests that the Pacific samples (Sites 871 and 872) are better preserved than those from the Atlantic (Site 1264).

Samples consisting of ~12 mg of single-species planktonic foraminifera were crushed between glass slides under the microscope, ensuring that all chambers were opened, and each was divided into 5 sub-samples

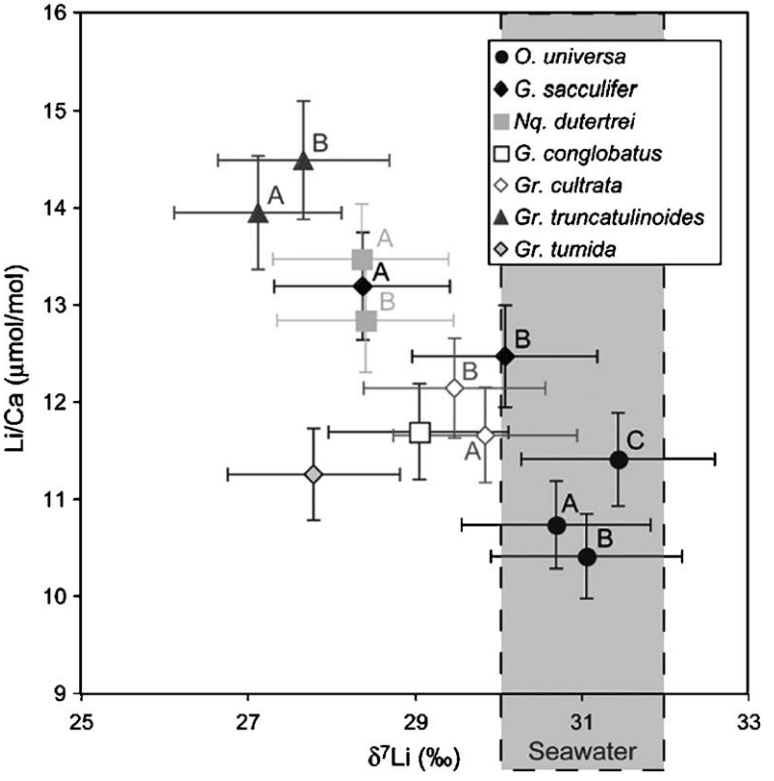

Fig. 1. δ^7Li and Li/Ca of recent planktonic foraminifera. *Globorotalia truncatulinoides* were picked from the >500 µm fraction; the mean annual sea surface temperature (SST) at the location of sample (A) is 28 °C and sample (B) is 19 °C [61]. *Orbulina universa* from the sample locality with a mean annual SST of 28 °C were picked from the >710 µm fraction (A) and the 710–500 µm fraction (B); those from the sample locality with a SST of 19 °C were picked from the >500 µm fraction (C). All other species were picked from the sample with a mean annual SST of 28 °C. Samples of *Neogloboquadrina dutertrei* were picked from the >500 µm fraction (A), and the 500–355 µm fraction (B). *Globigerinoides sacculifer* was picked from the >500 µm fraction (A) and the 500–355 µm fraction (B). *Globorotalia cultrata* was picked from the >710 µm (A) and the 710–500 µm fraction (B). The dashed vertical lines represent the best estimate for modern seawater δ^7Li, including the standard deviation [9]. Error bars are the external error (2σ).

for cleaning. Crushed tests were cleaned firstly by ultrasonication in water and methanol to remove adhering particles and clays, secondly by reductive cleaning to remove ferromanganese coatings, thirdly by oxidation to remove organics, and finally by weak acid leaching to remove any re-absorbed ions [38,39]. The sample was then dissolved in ~400 μl of 0.15 M thermally distilled (TD) HNO_3. This protocol was adopted after extensive testing of the effects of cleaning techniques on the chemical composition of different species of foraminifera [40]. Although reductive cleaning was not found necessary to obtain reliable Li/Ca and δ^7Li values, it was performed on all samples to facilitate the collection of other data, such as Mg/Ca (e.g. [41]).

Trace element/Ca ratios were determined by ICP–MS (Agilent™ 7500 series), following the procedure given in Rosenthal et al. [42]. The Ca concentration of the sample was determined first, and then matched to that of the standards, which were prepared gravimetrically from high purity single element standard solutions (Romil™ or Alfa Aesar™). The detection limit was 34 ppt for Li, compared to ~1 ppb in the sample

Table 2
Lithium isotope, Li/Ca, Mg/Ca and Sr/Ca data for recent and ancient planktonic foraminifera samples. Sediment samples M35010-2 and GIK15672-2 are from, respectively, ~19°N and ~35°N, in the North Atlantic

Species	Size fraction (μm)	Sediment sample	Age (Ma)	δ^7Li (‰)	Li/Ca (μmol/mol)	Corrected Li/Ca	Mg/Ca (mmol/mol)	Sr/Ca (mmol/mol)
Recent samples								
Orbulina universa	>710	M35010-2	–	30.7	10.7	–	8.51	1.29
Orbulina universa	710–500	M35010-2	–	31.1	10.4	–	8.54	1.33
Orbulina universa	>500	GIK15672-2	–	31.4	11.4	–	5.33	1.32
Globigerinoides sacculifer	>500	M35010-2	–	28.4	13.2	–	4.35	1.38
Globigerinoides sacculifer	500–355	M35010-2	–	30.1	12.5	–	4.18	1.36
Neogloboquadrina dutertrei	>500	M35010-2	–	28.4	13.5	–	3.05	1.40
Neogloboquadrina dutertrei	500–355	M35010-2	–	28.4	12.8	–	2.69	1.37
Globigerinoides conglobatus	>500	M35010-2	–	29.0	11.7	–	3.05	1.33
Globorotalia cultrata	>710	M35010-2	–	29.8	11.7	–	2.59	1.30
Globorotalia cultrata	710–500	M35010-2	–	29.5	12.1	–	2.86	1.33
Globorotalia truncatulinoides	>500	M35010-2	–	27.1	13.9	–	2.20	1.40
Globorotalia truncatulinoides	>500	GIK15672-2	–	27.7	14.5	–	1.57	1.38
Globorotalia tumida	>500	M35010-2	–	27.8	11.3	–	2.14	1.32
Ancient samples								
Orbulina	>500	ODP 871A 3H2 123–125	3.00	30.9	7.12	–	3.81	1.20
Orbulina	>355	ODP 871A 3H5 60–62	6.00	29.7	6.26	–	3.36	1.06
Orbulina	>355	ODP 872C 5H2 14–16	9.02	–	7.80	–	3.33	1.16
Orbulina	>355	ODP 872C 6H5 20–22	11.40	29.7	8.86	–	3.79	1.16
Orbulina	500–355	ODP 871A 4H5 59–61	11.81	29.3	–	–	4.80	1.27
Orbulina	>500	ODP 872C 5H6 59–61	10.39	–	8.56	–	3.95	1.17
Orbulina	500–355	ODP 1264A 14H5 140–150	10.49	28.6	8.85	–	2.39	1.17
Orbulina	500–355	ODP 1264A 13H5 140–150	9.56	28.7	8.25	–	2.20	1.23
Orbulina	500–355	ODP 1264A 11H5 140–150	8.35	29.9	7.18	–	1.84	1.12
Orbulina	500–355	ODP 1264A 1H5 145–150	1.78	30.0	8.37	–	2.40	1.28
Globorotalia cultrata	>500	ODP 871A 2H2 59–61	0.98	28.7	9.32	8.44	2.61	1.23
Globoquadrina altispira	>500	ODP 871A 7H2 124–126	14.73	26.6	12.3	9.55	3.35	1.38
Globoquadrina altispira	>500	ODP 871A 6H6 60–62	13.06	27.6	12.0	9.30	3.46	1.35
Globoquadrina altispira	>500	ODP 871A 4H5 59–61	11.81	27.5	12.1	9.36	3.18	1.28
Globoquadrina altispira	>500	ODP 872C 11H6 20–22	18.38	27.6	12.7	9.85	4.10	1.28
Globoquadrina venezuelana	>500	ODP 1264A 18H2 127–129	13.15	27.0	12.6	10.2	2.05	1.23
Globoquadrina venezuelana	500–355	ODP 1264A 18H2 127–129	13.15	25.2	11.2	9.11	1.88	1.24
Globoquadrina venezuelana	>355	ODP 1264A 20H5 140–150	18.34	27.9	11.5	9.32	2.62	1.39
Globoquadrina venezuelana	500–355	ODP 1264A 19H5 140–150	16.24	25.6	11.6	9.44	2.43	1.27
Globoquadrina venezuelana	>500	ODP 1264A 18H5 140–150	14.14	26.2	12.0	9.70	1.98	1.25
Globoquadrina venezuelana	500–355	ODP 1264A 17H5 140–150	12.14	26.6	11.6	9.36	1.90	1.25
Globoquadrina venezuelana	500–355	ODP 1264A 16H5 140–150	11.02	27.8	11.1	9.00	2.12	1.23
Globoquadrina venezuelana	>500	ODP 1264A 14H5 140–150	10.49	29.0	10.8	8.78	2.04	1.21
Globoquadrina venezuelana	>500	ODP 1264A 13H5 140–150	9.56	28.2	10.3	8.32	1.99	1.25

solution. The external reproducibility of Li/Ca, Mg/Ca and Sr/Ca is, respectively, 4.2%, 1.7% and 2.4% (2σ, where σ is the standard deviation), based on repeat (n=10) analysis of a large sample of single species foraminifera.

For Li isotope analysis, an aliquot of the sample solution containing ~4 ng Li was loaded onto ~4.3 ml of AG50W-X8 (Bio-Rad™) cation exchange resin and eluted with 0.2 M TD HCl to separate Li [43]. Lithium isotope ratios were determined on ~6 ppb solutions by MC–ICP–MS (Nu Instruments™) using a sample-standard bracketing technique. Full details of this method are given in Kisakürek et al. [16]. Li isotope ratios are reported as δ^7Li values, relative to the NIST LSVEC Li_2CO_3 standard [44]:

$$\delta^7\mathrm{Li} = \left[\frac{(^7\mathrm{Li}/^6\mathrm{Li})_{\mathrm{sample}} - (^7\mathrm{Li}/^6\mathrm{Li})_{\mathrm{standard}}}{(^7\mathrm{Li}/^6\mathrm{Li})_{\mathrm{standard}}}\right] \times 100$$

The external reproducibility of the Li isotope analyses is ±1‰ (2σ), based on repeat (n=6) measurements of a large sample of single species foraminifera. The total procedural blank was 12 pg Li, which is insignificant in relation to the sample size (<0.3%).

3. Results

Analyses of recent (core-top) foraminifera (Fig. 1 and Table 2) indicate that the species *Orbulina universa* effectively archives the Li isotope ratio of modern seawater; a similar result has also been reported recently [45]. Other species record different δ^7Li (and Li/Ca) values, but the offset from seawater is reproducible. With the exception of *Globorotalia tumida*, foraminiferal δ^7Li and Li/Ca appear to fall on a mixing line. This is potentially of interest for understanding mechanisms of biomineralization, but it is not the focus of this contribution. Neither δ^7Li nor Li/Ca show any significant variation with test size (at least for tests >355 μm), with the exception of *Globigerinoides sacculifer*. Foraminiferal δ^7Li does not vary with calcification temperature, but Li/Ca appears to decrease very slightly (~0.17 μmol/mol/°C) as calcification temperature increases (Fig. 2). However, other more extensive data sets do not show significant variation between foraminiferal Li/Ca and calcification temperature at the 95% confidence level (Fig. 2), and Delaney et al. [46] also failed to find a temperature effect on the Li/Ca ratio of cultured planktonic foraminifera.

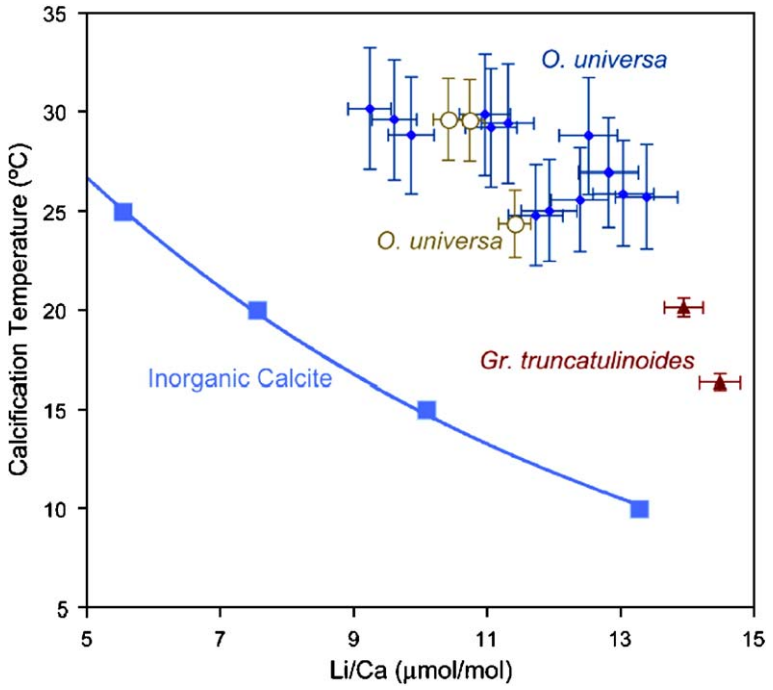

Fig. 2. Effect of temperature on Li/Ca of foraminiferal calcite. Open circles are data from this study; closed diamonds are from Hall and Chan [33] excluding data from north of 50°N. Data for inorganic calcite are shown for comparison [62]; these have been adjusted to seawater salinity after Marriott et al. [63]. Calcification temperature of foraminiferal calcite was calculated from Mg/Ca using the calibrations of Anand et al. [32]. Error bars are the external error (2σ).

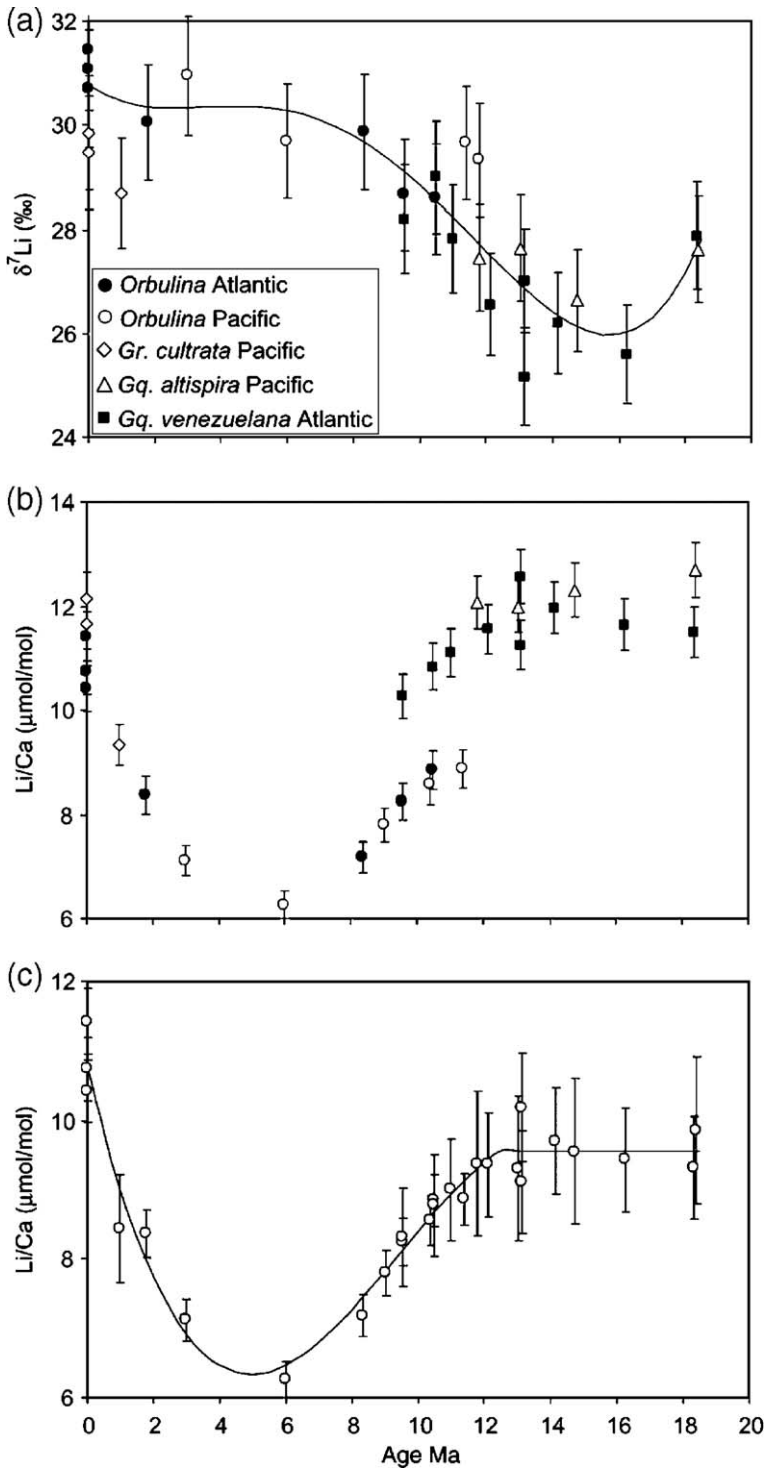

Fig. 3. Temporal record of (a) foraminiferal δ^7Li, (b) foraminiferal Li/Ca, and (c) foraminiferal Li/Ca corrected for species effects (see text for details). Solid lines show the least squares fit to the data (MATLAB® Curve Fitting Tool), such that R^2 is >0.8. These curve fits have been used in all subsequent calculations. Error bars are the external error (2σ).

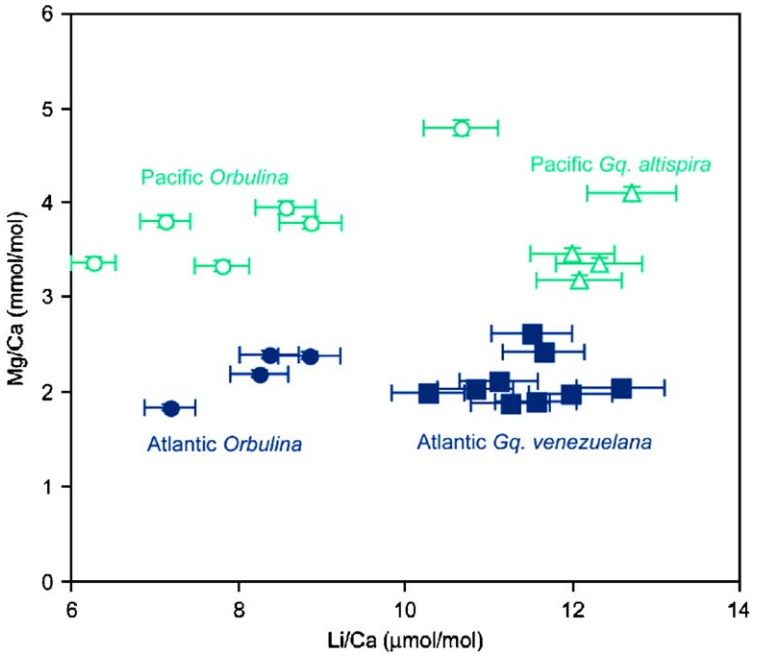

Fig. 4. Li/Ca and Mg/Ca of ancient planktonic foraminifera. Foraminifera from the equatorial west Pacific have higher Mg/Ca than those from the sub-tropical South Atlantic. Assuming that the Mg/Ca ratio of seawater has remained constant, and using the Mg/Ca vs. temperature calibrations reported in Anand et al. [32], this indicates that calcification temperatures at the Pacific site (~20 °C) have been higher than at the Atlantic site (~14 °C) since 18 Ma. Meanwhile, Li/Ca shows a similar range for both locations. The lack of correlation between Mg/Ca and Li/Ca suggests that temperature has had a negligible effect on the Li/Ca records. Error bars are the external error (2σ).

Temporal records of foraminiferal Li/Ca and δ^7Li from the western equatorial Pacific and the subtropical south Atlantic are shown in Fig. 3. The two sites have different diagenetic histories, different average sea-surface temperatures (Fig. 4) and different seawater [CO_3^{2-}], yet the consistency of the data is remarkable. This indicates that the foraminifera are recording global seawater Li chemistry, and that secondary effects on foraminiferal Li/Ca and δ^7Li are minimal. Species effects are within the analytical uncertainty for δ^7Li, but they are apparent in the Li/Ca record. Therefore we have applied a simple species adjustment to our Li/Ca data by normalizing all species to *O. universa*; these adjusted values are also shown in Fig. 3c and Table 2.

Foraminiferal δ^7Li increased from ~25 to ~30‰ between ~16 and ~8 Ma, and has remained close to ~30‰ (i.e. the present-day value for seawater) since that time. *Orbulina*-normalised Li/Ca remained close to ~9.5 µmol/mol between ~18 and ~12 Ma, decreased to ~6 µmol/mol at ~6 Ma, and then increased to the present-day value of ~11 µmol/mol.

It is interesting to note that foraminiferal Sr/Ca (Table 2) is significantly correlated ($p<0.05$) with foraminiferal Li/Ca, and that our records for planktonic species show a similar pattern to the benthic foraminiferal Sr/Ca record recently published by Lear et al. [47]. While both Li and Sr are principally added to the oceans via rivers and hydrothermal fluids, they have different sinks. Li is mainly taken up into clays and basalt (Table 1) while Sr is mostly taken up by carbonates (e.g. [47]). Given that secondary effects on these trace element/Ca records from different locations are unlikely to have been the same, the consistency between these records suggests that changes in seawater Li/Ca and Sr/Ca during this period were principally driven by changes in their input fluxes.

4. Discussion

4.1. Variation in seawater Li and δ^7Li

Changes in the amount and isotopic composition of Li in seawater result from long-term imbalances in weathering and hydrothermal inputs and sedimentary outputs. This relationship is expressed in the equation below written in terms of Li (Eq. (1)) and δ^7Li (Eq. (2)) (e.g. [47–50]):

$$\frac{\partial M_{\mathrm{Li}}}{\partial t} = F_{\mathrm{RIV}}^{\mathrm{Li}} + F_{\mathrm{HYD}}^{\mathrm{Li}} - F_{\mathrm{SED}}^{\mathrm{Li}} \quad (1)$$

$$M_{\mathrm{Li}} \times \frac{\partial \delta^7\mathrm{Li}_{\mathrm{SW}}}{\partial t} = F^{\mathrm{Li}}_{\mathrm{RIV}}(\delta^7\mathrm{Li}_{\mathrm{RIV}} - \delta^7\mathrm{Li}_{\mathrm{SW}}) + F^{\mathrm{Li}}_{\mathrm{HYD}}(\delta^7\mathrm{Li}_{\mathrm{HYD}} - \delta^7\mathrm{Li}_{\mathrm{SW}}) - F^{\mathrm{Li}}_{\mathrm{SED}}(\Delta_{\mathrm{SED}}) \quad (2)$$

where M_{Li} is the total number of moles of Li in the ocean and F^{Li} is the Li flux in/out of seawater (subscript SW) from rivers, hydrothermal fluids and sediments (subscripts RIV, HYD and SED, respectively). Δ_{SED} is the average δ^7Li offset between marine sediments and the seawater [Li^+].

While the foraminiferal δ^7Li record corresponds to seawater δ^7Li (so the data presented in Fig. 3a are described by Eq. (2)), interpretation of the foraminiferal Li/Ca record in terms of seawater Li (Eq. (1)) is more complicated because we need to know (i) the partition coefficient, D, where $D=(\mathrm{Li/Ca})_{\mathrm{foram}}/(\mathrm{Li/Ca})_{\mathrm{seawater}}$ and, (ii) how the seawater Ca concentration has changed in the past. D can be derived from analyses of recent *Orbulina* (Fig. 1) and is $\sim 4.2\times10^{-3}$. Estimates of the past variation in seawater [Ca^{2+}] are shown in Fig. 5a and have been obtained from analysis of marine halite fluid inclusions [51] as well as records of seawater δ^{44}Ca [52,53]. The range of these estimates is large; the effect of this uncertainty on the seawater Li curve is shown in Fig. 5b.

Given that seafloor spreading rates have not changed significantly since 20 Ma and potentially even further back in Earth's history (e.g. [54]), it can be assumed that

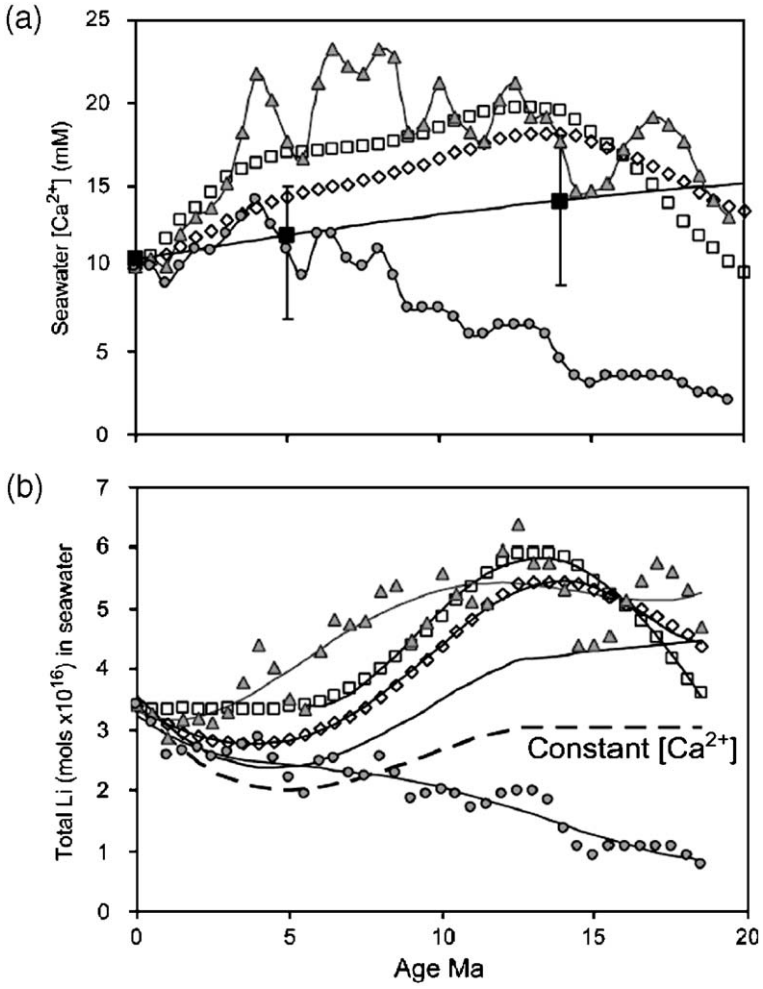

Fig. 5. Temporal record of (a) seawater [Ca^{2+}]. Data are from Heuser et al. [52] (open squares, scenario 1; open diamonds, scenario 2), Horita et al. [51] (closed squares) and Fantle and DePaolo [53] (triangles, $\delta^{44}Ca_{RIV}=-0.57‰$; circles, $\delta^{44}Ca_{RIV}=-0.39‰$). (b) Variation in the total amount of Li in the ocean. Symbols are the same as in (a); the dashed line assumes that seawater [Ca^{2+}] has remained unchanged. Solid lines denote the least squares fit through the data (MATLAB® Curve Fitting Tool) (R^2 is >0.9, except for the triangles from [53], for which R^2 is 0.77). These curves have been used to generate the records shown in Fig. 7.

both the high-temperature hydrothermal flux of Li to the oceans, and the rate of removal of Li due to low-temperature alteration of basalt, have been relatively constant during this period. Variations in seawater δ^7Li and Li during the past 20 Ma are therefore likely due to variations in (i) Δ_{SED}, (ii) the rate of removal of Li into marine sediments, or (iii) continental weathering. Changes in the first two parameters over the past 20 Ma are unlikely because, in the case of (i), there is a well-defined linear correlation between δ^7Li and the Li concentration of marine basalts aged between <1 and 46 Ma [13], and in the case of (ii), records of accumulation rates of non-carbonate material on the seafloor [55] suggest that periods of low accumulation (and therefore lower uptake of Li into sediments) broadly correspond to relatively low seawater Li, and vice-versa (Fig. 6). Changes in accumulation of non-carbonate material therefore acted to dampen the variability in seawater Li, if indeed this has had any affect at all. Thus, the over-arching control on changes in seawater Li and δ^7Li is variation in continental weathering.

4.2. Silicate weathering, atmospheric CO_2 and climate

Given a constant flux of Li into marine sediments and basalt and a constant flux (and δ^7Li value) of hydrothermal Li to the oceans (Table 1), together with a constant value for Δ_{SED} (−15‰ [11,13,14]), the variation in the isotopic composition and Li flux of rivers since 18 Ma can be calculated using Eqs. (1) and (2); results are shown in Fig. 7. Although the uncertainty in the record of seawater [Ca^{2+}] generates large uncertainties in both records, the general trends seem to be robust. The mean and standard deviation of the different modelled outputs is shown in Fig. 8a.

Fig. 8a indicates that between 16 and ~8 Ma, the river flux of dissolved Li decreased, which implies that silicate weathering rates decreased [19]. Over the same interval, the δ^7Li value of the river input increased which suggests that weathering also became less intense [15,16,18]. Observations of other tracers of continental weathering (Fig. 8c) also point to lower weathering fluxes around this time; there is a break in the slope of the seawater $^{87}Sr/^{86}Sr$ curve at ~16 Ma [4], and seawater $^{187}Os/^{188}Os$ becomes less radiogenic between ~16 Ma and ~10 Ma [56]. Two independent reconstructions of atmospheric carbon dioxide suggest that pCO_2 increased during this period (Fig. 8b); our data indicate that this could have been forced by a reduction in silicate weathering (although it should be noted that organic carbon burial is thought to have slowed over this interval, which could also facilitate an increase in pCO_2 [57]). Since ~8 Ma, the river flux of dissolved Li has

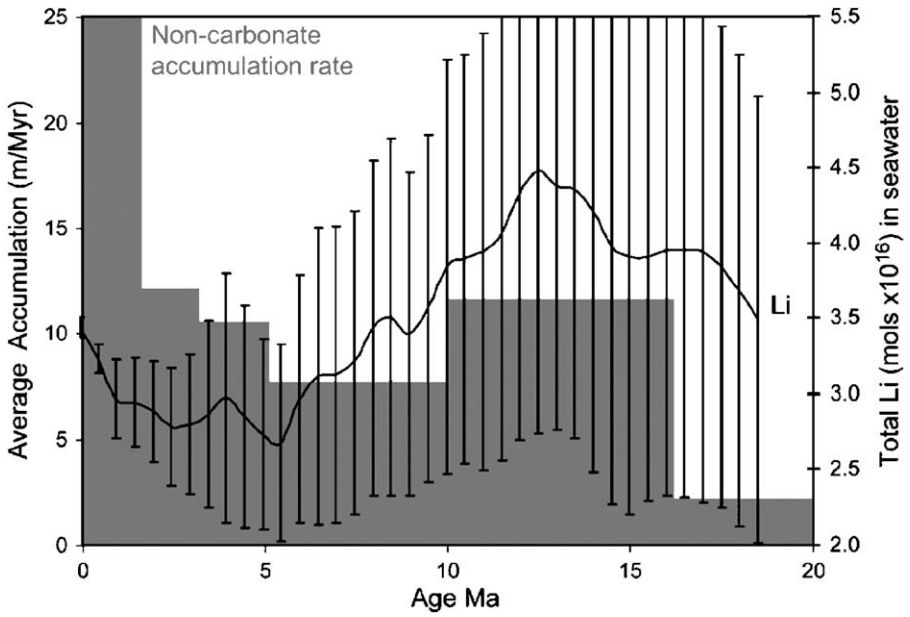

Fig. 6. Average rate of accumulation of non-carbonate material on the global seafloor over the past 20 Ma. Data are from Whitman and Davies [55] and age has been converted to the time scale of Berggren et al. [64]. Similar patterns of non-carbonate sediment accumulation have been observed more recently for the Bengal Fan [65], the central Indian Ocean [66] and Asian marginal seas [67]. The average and standard deviation of all of the seawater Li records shown in Fig. 5b is superimposed for comparison.

increased and its δ^7Li value has continued to increase. This implies an increase in silicate weathering rates, but a decrease in weathering intensity; this could be due to a shift to a more weathering-limited regime (e.g. [58]). Increased silicate weathering rates are also implied from the seawater $^{187}Os/^{188}Os$ record (Fig. 8c); seawater Os has become increasingly radiogenic since ~10 Ma suggesting increased continental input. An increase in the silicate weathering rate should result in the draw-down of atmospheric CO_2. However, it seems that pCO_2 has remained relatively stable since that time (Fig. 8b and [3]), suggesting that weathering processes are not presently solely responsible for forcing of atmospheric CO_2. Rather, any reduction in pCO_2 resulting from increased silicate weathering may have been compensated by a decrease in the burial of organic carbon [57]. What is intriguing is that, our seawater Li records, as well as records of seawater $^{87}Sr/^{86}Sr$ (e.g., [4]) and $^{187}Os/^{188}Os$ [56], imply that silicate weathering has increased since ~8 Ma despite global cooling and the onset of northern hemisphere glaciation at ~3 Ma. This suggests that silicate weathering has been decoupled from climate during this period. It is not clear why this has occurred, but it could be related to enhanced physical erosion (e.g. [59]) and/or the expansion of grasslands producing fine soils [60]. What is clear is that if we are to ascertain the ability of the Earth system to cope with anthropogenic CO_2 emissions, it is essential to better constrain the links between weathering and climate.

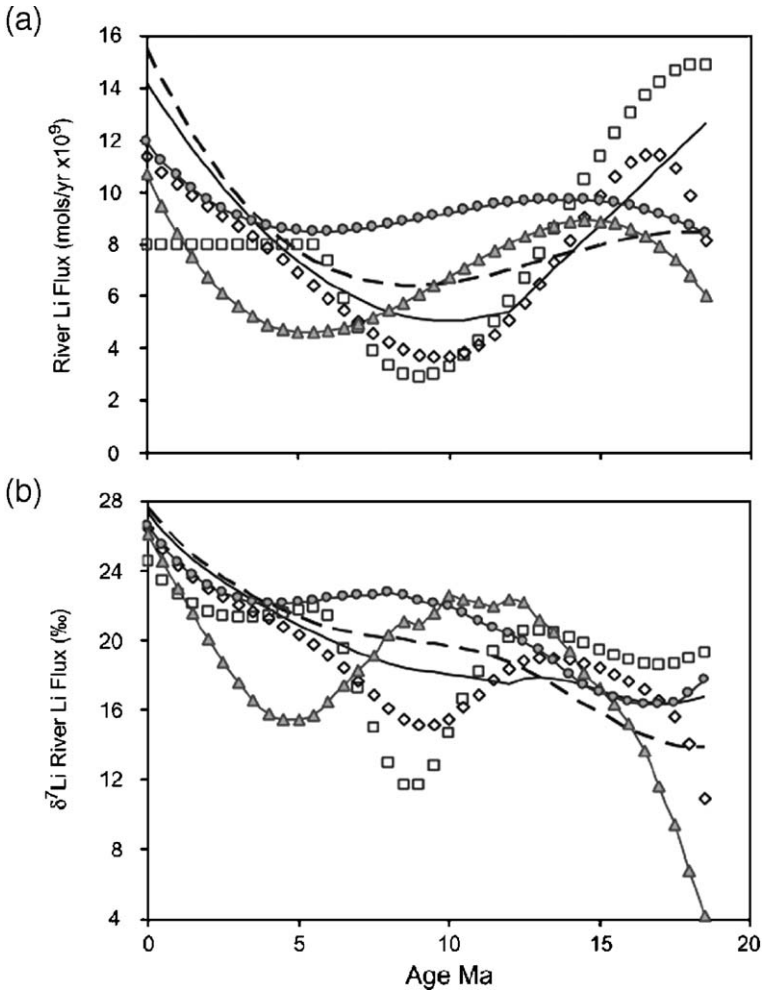

Fig. 7. Modelled temporal records of (a) the river Li flux and (b) the δ^7Li value of the river flux. Symbols are the same as for Fig. 5. Note that because of the apparent variation in $[Ca^{2+}]$ the modelled value for the present day river flux and the modelled δ^7Li value for the present day river Li flux are higher than reported in Table 1 (with the exception of calculations based on scenario 1 from [52]).

5. Conclusions

This study demonstrates that measurements of Li/Ca and δ^7Li of ancient planktonic foraminifera can be used to reconstruct past changes in the Li isotope composition and Li/Ca ratio of seawater. Given that hydrothermal and output fluxes have remained constant, and assuming scenarios of changing seawater calcium

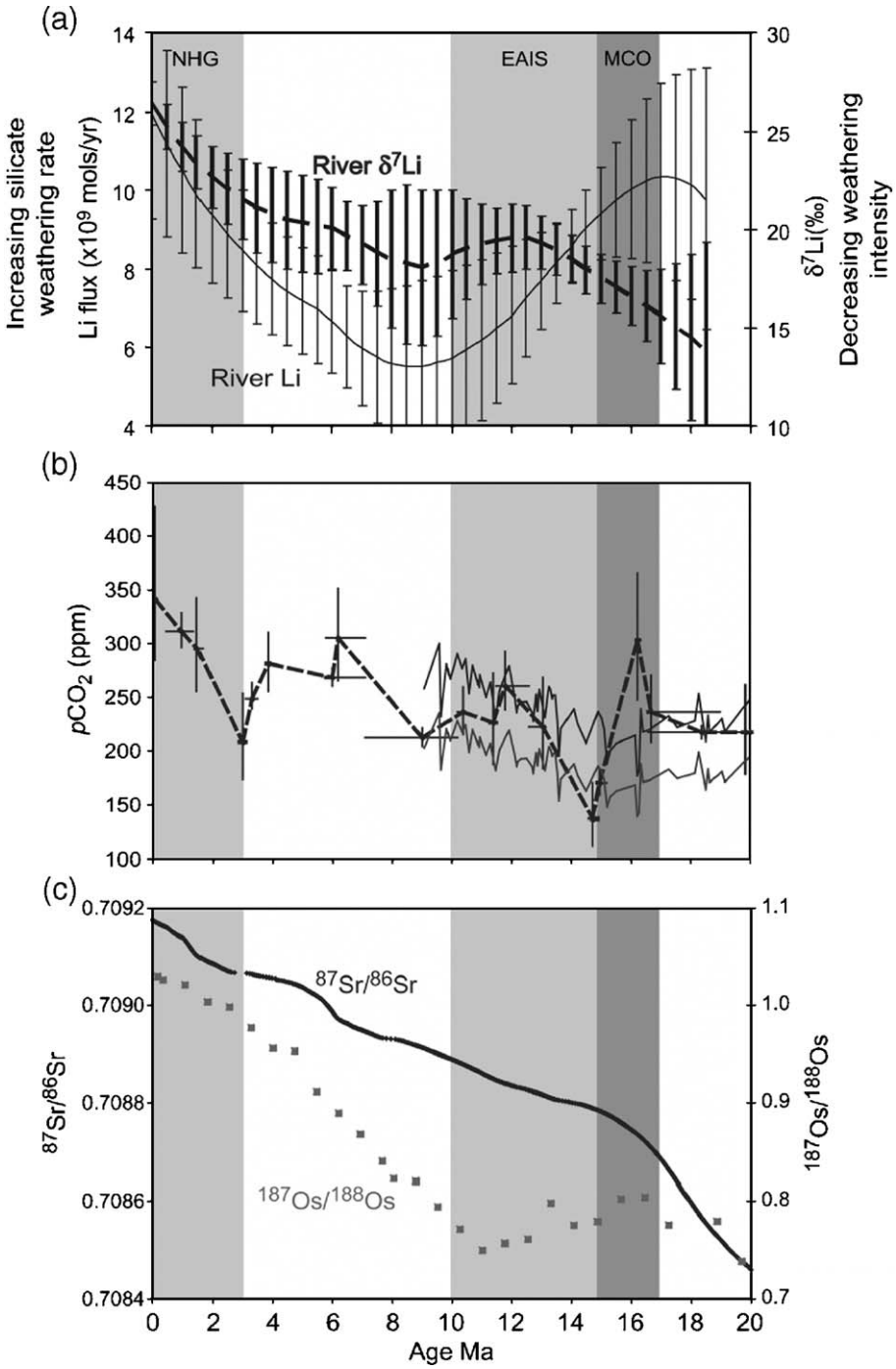

Fig. 8. Temporal records of (a) averaged riverine Li flux and isotopic composition (see text for details), (b) atmospheric pCO_2 (solid lines from Pagani et al. [68]; dashed lines from Pearson and Palmer [69]), and (c) seawater $^{87}Sr/^{86}Sr$ [4] and $^{187}Os/^{188}Os$ [56]. Generalised climatic periods [1] are shown by vertical bars: MCO=Miocene Climatic Optimum, EAIS=East Antarctic Ice Sheet expansion, NHG=Northern Hemisphere Glaciation.

concentrations, first order approximations of riverine δ^7Li and river Li flux for the past 18Ma are obtained. River Li flux is interpreted in terms of continental silicate weathering rate, while river δ^7Li is interpreted in terms of silicate weathering intensity. Our records suggest that both silicate weathering rates and weathering intensity decreased between 16 and ~8 Ma which may have been responsible for putative increases in levels of atmospheric CO_2. In contrast, silicate weathering rates appear to have increased since ~8 Ma despite global cooling and apparently little variation in atmospheric CO_2.

Acknowledgments

We are very grateful to Harry Elderfield, Lui-Heung Chan and one anonymous reviewer for their careful reading and constructive comments which have greatly improved this manuscript.

We would like to thank Paul Pearson, the GEOMAR Lithothek and the Ocean Drilling Program for providing the samples used in this work. We would also like to thank Charlotte Brunner for thorough taxonomic training, and Kevin Burton, Nigel Harris and Gideon Henderson for constructive comments on an early version of this manuscript. ECH was funded by NERC studentship NER/S/A/2000/03506 and participation on ODP Leg 208 was funded by the UKODP programme.

References

[1] J. Zachos, M. Pagani, L. Sloan, E. Thomas, K. Billups, Trends, rhythms, and aberrations in global climate 65 Ma to Present, Science 292 (2001) 686–693.

[2] J.R. Petit, J. Jouzel, D. Raynaud, N.I. Barkov, J.-M. Barnola, I. Basile, M. Bender, J. Chappellaz, M. Davis, G. Delaygue, M. Delmotte, V.M. Kotlyakov, M. Legrand, V.Y. Lipenkov, C. Lorius, L. Pépin, C. Ritz, E. Saltzman, M. Stievenard, Climate and atmospheric history of the past 420,000 years from the Vostock Ice Core, Antarctica, Nature 399 (1999) 429–436.

[3] M. Pagani, J.C. Zachos, K.H. Freeman, B. Tipple, S. Bohaty, Marked decline in atmospheric carbon dioxide concentrations during the Paleogene, Science 309 (2005) 600–603.

[4] J.M. McArthur, R.J. Howarth, T.R. Baily, Strontium isotope stratigraphy: LOWESS version 3: best fit to the marine Sr-isotope curve for 0–509 Ma and accompanying look-up table for deriving numerical age, J. Geol. 109 (2001) 155–170.

[5] M.E. Raymo, W.F. Ruddiman, Tectonic forcing of late Cenozoic climate, Nature 359 (1992) 117–122.

[6] L. Oliver, N. Harris, M. Bickle, H. Chapman, N. Dise, M. Horstwood, Silicate weathering rates decoupled from the ^{87}Sr/^{86}Sr ratio of the dissolved load during Himalayan erosion, Chem. Geol. 201 (2003) 119–139.

[7] M.L. Delaney, E.A. Boyle, Lithium in foraminiferal shells: implications for high-temperature hydrothermal circulation fluxes and oceanic crustal generation rates, Earth Planet. Sci. Lett. 80 (1986) 91–105.

[8] Y. Huh, L.-H. Chan, L. Zhang, J.M. Edmond, Lithium and its isotopes in major world rivers: implications for weathering and the oceanic budget, Geochim. Cosmochim. Acta 62 (1998) 2039–2051.

[9] P.B. Tomascak, Developments in the understanding application of lithium isotopes in the Earth and Planetary Sciences, Rev. Min. Geochem. 55 (2004) 153–195.

[10] A.M. Bray, L.-H. Chan, K.L. Von Damm, Constancy of the Li-isotopic signature in mid-ocean ridge hydrothermal fluids: evidence for equilibrium control, Eos Trans. AGU 82 (2001) OS41A-0440.

[11] L. Zhang, L.-H. Chan, J.M. Gieskes, Lithium isotope geochemistry of pore waters from Ocean Drilling Program Sites 918 and 919, Irminger Basin, Geochim. Cosmochim. Acta 62 (1998) 2437–2450.

[12] J. Hoefs, M. Sywall, Lithium isotope composition of Quaternary and Tertiary biogenic carbonates and a global lithium isotope balance, Geochim. Cosmochim. Acta 61 (1997) 2679–2690.

[13] L.-H. Chan, J.M. Edmond, G. Thompson, K. Gillis, Lithium isotopic composition of submarine basalts: implications for the lithium cycle in the oceans, Earth Planet. Sci. Lett. 108 (1992) 151–160.

[14] J.S. Pistiner, G.M. Henderson, Lithium-isotope fractionation during continental weathering processes, Earth Planet. Sci. Lett. 214 (2003) 327–339.

[15] Y. Huh, L.-H. Chan, J.M. Edmond, Lithium isotopes as a probe of weathering processes: Orinoco River, Earth Planet. Sci. Lett. 194 (2001) 189–199.

[16] B. Kisakürek, M. Widdowson, R.H. James, Behaviour of Li isotopes during continental weathering: the Bidar laterite profile, India, Chem. Geol. 212 (2004) 27–44.

[17] H.W. Nesbitt, G.M. Young, Early Proterozoic climates and plate motions inferred from major element chemistry of lutites, Nature 299 (1982) 715–717.

[18] N. Vigier, K.W. Burton, S.R. Gislason, N.W. Rogers, B.F. Schaefer, R.H. James, Constraints on basalt erosion from Li isotopes and U-series nuclides measured in Icelandic rivers, Geochim. Cosmochim. Acta 66 (2002) A806.

[19] B. Kisakürek, R.H. James, N.B.W. Harris, Li and δ^7Li in Himalayan rivers: proxies for silicate weathering, Earth Planet. Sci. Lett. 237 (2005) 387–401.

[20] P. Stoffyn-Egli, F.T. Mackenzie, Mass balance of dissolved lithium in the oceans, Geochim. Cosmochim. Acta 48 (1984) 859–872.

[21] L.-H. Chan, J.C. Alt, D.A.H. Teagle, Lithium and lithium isotope profiles through the upper oceanic crust: a study of seawater–basalt exchange at ODP Sites 504B and 896A, Earth Planet. Sci. Lett. 201 (2002) 187–201.

[22] C.F. You, L.-H. Chan, A.J. Spivack, J.M. Gieskes, Lithium, boron, and their isotopes in sediments and pore waters of Ocean Drilling Program Site 808, Nankai Trough: Implications for fluid expulsion in accretionary prisms, Geology 23 (1995) 37–40.

[23] L.-H. Chan, M. Kastner, Lithium isotopic compositions of pore fluids and sediments in the Costa Rica subduction zone: implications for fluid processes and sediment contribution to the arc volcanoes, Earth Planet. Sci. Lett. 183 (2000) 275–290.

[24] J.B. Martin, M. Kastner, H. Elderfield, Lithium: sources in pore fluids of Peru slope sediments and implications for oceanic fluxes, Mar. Geol. 102 (1991) 281–292.

[25] W.E. Seyfried, D.R. Janecky, M.J. Mottl, Alteration of the oceanic crust: implications for geochemical cycles of lithium and boron, Geochim. Cosmochim. Acta 48 (1984) 557–569.
[26] C.G. Wheat, M.J. Mottl, Composition of pore and spring waters from Baby Bare: global implications of geochemical fluxes from a ridge flank hydrothermal system, Geochim. Cosmochim. Acta 64 (2000) 629–642.
[27] L.-H. Chan, L. Zhang, J.R. Hein, Lithium isotope characteristics of marine sediments, EOS 75 (1994) 314.
[28] M. Kastner, H. Elderfield, J.B. Martin, Fluids in convergent margins: what do we know about their composition, origin, role in diagenesis and importance for oceanic chemical fluxes? Philos. Trans. R. Soc. Lond., A 335 (1991) 243–259.
[29] J.P. Foucher, X. Le Pichon, S. Lallemant, M.A. Hobart, P. Henry, M. Benedetti, G.K. Westbrook, M.G. Langseth, Heat flow, tectonics, and fluid circulation at the toe of the Barbados Ridge accretionary prism, J. Geophys. Res. 95 (1990) 8859–8867.
[30] B. Carson, E. Suess, J.C. Strasser, Fluid flow and mass flux determinations at vent sites on the Cascadia Margin accretionary prism, J. Geophys. Res. 95 (1990) 8891–8897.
[31] D.M. Saffer, E.J. Screaton, Fluid flow at the toe of convergent margins: interpretation of sharp pore-water geochemical gradients, Earth Planet. Sci. Lett. 213 (2003) 261–270.
[32] P. Anand, H. Elderfield, M.H. Conte, Calibration of Mg/Ca thermometry in planktonic foraminifera from a sediment trap time series, Paleoceanography 18 (2003) 1050.
[33] J.M. Hall, L.-H. Chan, Li/Ca in multiple species of benthic and planktonic foraminifera: thermocline, latitudinal, and glacial–interglacial variation, Geochim. Cosmochim. Acta 68 (2004) 529–545.
[34] P.B. Tomascak, R.W. Carlson, S.B. Shirey, Accurate and precise determination of Li isotopic compositions by multi-collector sector ICP–MS, Chem. Geol. 158 (1999) 145–154.
[35] W.F. Ruddiman, Investigations of Quaternary climate based on planktonic foraminifera, in: A.T.S. Ramsay (Ed.), Oceanic Micropalaeontology, Academic Press, London, 1977, pp. 101–161.
[36] P.N. Pearson, Planktonic foraminifer biostratigraphy and the development of pelagic caps on guyots in the Marshall Islands group, in: J.A. Haggerty, I. Premoli Silva, F. Rack, M.K. McNutt (Eds.), Proceedings of the Ocean Drilling Program, Scientific Results, vol. 144, Ocean Drilling Program, College Station, TX, 1995, pp. 21–59.
[37] Shipboard_Scientific_Party, Site 1264, in: J. Zachos, D. Kroon, P. Blum (Eds.), Proceedings of the Ocean Drilling Program Initial Reports, vol. 208, Ocean Drilling Program, College Station TX, 2004, Available from World Wide Web: http://www-odp.tamu.edu/publications/208_IR/208ir.htm.
[38] E.A. Boyle, L.D. Keigwin, Comparison of Atlantic and Pacific paleochemical records for the last 215,000 years: changes in deep ocean circulation and chemical inventories, Earth Planet. Sci. Lett. 76 (1985/86) 135–150.
[39] Y. Rosenthal, E.A. Boyle, L. Labeyrie, Last glacial maximum paleochemistry and deepwater circulation in the Southern Ocean: evidence from foraminiferal cadmium, Paleoceanography 12 (1997) 787–796.
[40] E.C. Hathorne, The trace element and lithium isotope composition of planktonic foraminifera, PhD, The Open University, (2004).
[41] P.A. Martin, D.W. Lea, A simple evaluation of cleaning procedures on fossil benthic foraminiferal Mg/Ca, Geochem. Geophys. Geosyst. 3 (2002) 10.1029.
[42] Y. Rosenthal, M.P. Field, R.M. Sherrell, Precise determination of element/calcium ratios in calcareous samples using sector field inductively coupled plasma mass spectrometry, Anal. Chem. 71 (1999) 3248–3253.
[43] R.H. James, M.R. Palmer, The lithium isotope composition of international rock standards, Chem. Geol. 166 (2000) 319–326.
[44] G.D. Flesch, A.R.J. Anderson, H.J. Svec, A secondary isotopic standard for $^{6}Li/^{7}Li$ determinations, Int. J. Mass Spectrom. 12 (1973) 265–272.
[45] J.M. Hall, L.-H. Chan, W.F. McDonough, K.K. Turekian, Determination of the lithium isotopic composition of planktonic foraminifera and its application as a paleo-seawater proxy, Mar. Geol. 217 (2005) 255–265.
[46] M.L. Delaney, A.W.H. Bé, E.A. Boyle, Li, Sr, Mg and Na in foraminiferal calcite shells from laboratory culture, sediment traps, and sediment cores, Geochim. Cosmochim. Acta 49 (1985) 1327–1341.
[47] C.H. Lear, H. Elderfield, P.A. Wilson, A Cenozoic seawater Sr/Ca record from benthic foraminiferal calcite and its application in determining global weathering fluxes, Earth Planet. Sci. Lett. 208 (2003) 69–84.
[48] C.L. De La Rocha, D.J. DePaolo, Isotopic evidence for variations in the marine calcium cycle over the Cenozoic, Science 289 (2000) 1176–1178.
[49] F.M. Richter, K.K. Turekian, Simple models for the geochemical response of the ocean to climatic and tectonic forcing, Earth Planet. Sci. Lett. 119 (1993) 121–131.
[50] A. Paytan, M. Kastner, D. Campbell, M.H. Thiemens, Seawater sulfur isotope fluctuations in the Cretaceous, Science 304 (2004) 1663–1665.
[51] J. Horita, H. Zimmermann, H.D. Holland, Chemical evolution of seawater during the Phanerozoic: implications from the record of marine evaporites, Geochim. Cosmochim. Acta 66 (21) (2002) 3733–3756.
[52] A. Heuser, A. Eisenhauer, F. Bohm, K. Wallmann, N. Gussone, P. N. Pearson, T.F. Nagler, W.-D. Dullo, Calcium isotope ($\delta^{44/40}Ca$) variations of Neogene planktonic foraminifera, Paleoceanography 20 (2005) PA2013.
[53] M.S. Fantle, D.J. DePaolo, Variations in the marine Ca cycle over the past 20 million years, Earth Planet. Sci. Lett. 237 (2005) 102–117.
[54] D.B. Rowley, Rate of plate creation and destruction: 180 Ma to Present, GSA Bull. 114 (2002) 927–933.
[55] J.M. Whitman, T.A. Davies, Cenozoic oceanic sedimentation rates: how good are the data? Mar. Geol. 30 (1979) 269–284.
[56] K.W. Burton, Global weathering variations inferred from marine radiogenic isotope records, J. Geochem. Explor. 88 (2006) 262–265.
[57] L.A. Derry, C. France-Lanord, Neogene growth of the sedimentary organic carbon reservoir, Paleoceanography 11 (1996) 267–275.
[58] L.R. Kump, S.L. Brantley, M.A. Arthur, Chemical weathering, atmospheric CO_2, and climate, Annu. Rev. Earth Planet. Sci. 28 (2000) 611–667.
[59] Z. Peizhen, P. Molnar, W.R. Downs, Increased sedimentation rates and grain sizes 2–4 Myr ago due to the influence of climate change on erosion rates, Nature 410 (2001) 891–897.
[60] G.J. Retallack, Cenozoic expansion of grasslands and climate cooling, J. Geol. 109 (2001) 407–426.
[61] S. Levitus, T.P. Boyer, World Ocean Atlas, Temperature, NOAA Atlas NESDIS, National Ocean and Atmospheres Administration, Silver Spring, Md, 1994.

[62] C.S. Marriott, G.M. Henderson, N.S. Belshaw, A.W. Tudhope, Temperature dependence of δ^7Li, δ^{44}Ca and Li/Ca during growth of calcium carbonate, Earth Planet. Sci. Lett. 222 (2004) 615–624.

[63] C.S. Marriott, G.M. Henderson, R. Crompton, M. Staubwasser, S. Shaw, Effect of mineralogy, salinity, and temperature on Li/Ca and Li isotope composition of calcium carbonate, Chem. Geol. 212 (2004) 5–15.

[64] W.A. Berggren, D.V. Kent, C.C. Swisher, M.-P. Aurby, A revised Cenozoic geochronology and chronostratigraphy, in: W.A. Berggren, D.V. Kent, C.C. Swisher, M.-P. Aurby, J. Hardenbol (Eds.), Geochronology, Time Scales and Global Stratigraphic Correlation, SPEM Special Publication, vol. 54, SPEM, 1995, pp. 129–212.

[65] D.W. Burbank, L.A. Derry, C. France-Lanord, Reduced Himalayan sediment production 8 Myr ago despite an intensified monsoon, Nature 364 (1993) 48–50.

[66] V.K. Banakar, A. Galy, N.P. Sukumaran, G. Parthiban, A.Y. Volvaiker, Himalayan sedimentary pulses recorded by silicate detritus within a ferromanganese crust from the Central Indian Ocean, Earth Planet. Sci. Lett. 205 (2003) 337–348.

[67] P.D. Clift, Controls on the erosion of Cenozoic Asia and the flux of clastic sediment to the ocean, Earth Planet. Sci. Lett. 241 (2006) 571–580.

[68] M. Pagani, M.A. Arthur, K.H. Freeman, Miocene evolution of atmospheric carbon dioxide, Paleoceanography 14 (1999) 273–292.

[69] P.N. Pearson, M.R. Palmer, Atmospheric carbon dioxide concentrations over the past 60 million years, Nature 406 (2000) 695–699.